A plant traits-based approach in vegetation modeling

Verheijen, L.M.

2015

document version
Publisher's PDF, also known as Version of record

Chapter 3

Inclusion of ecologically based trait variation in plant functional types reduces the projected land carbon sink in an earth system model

Verheijen, L.M.[1], Aerts, R.[1], Brovkin, V.[2], Cavender-Bares, J.[3], Cornelissen, J.H.C.[1], Kattge, J.[4], Van Bodegom, P.M.[1,5]

[1]VU University Amsterdam, Systems Ecology, Department of Ecological Science, De Boelelaan 1085, 1081 HV Amsterdam, the Netherlands
[2]Max Planck Institute for Meteorology, Bundesstrasse 55, 20146 Hamburg, Germany
[3]University of Minnesota, Department of Ecology, Evolution and Behavior, Saint Paul, MN 55108, USA
[4]Max Planck Institute for Biogeochemistry, Hans Knoell Strasse 10, 07745 Jena, Germany
[5]Leiden University, Institute of Environmental Sciences, Einsteinweg 2, 2333 CC, Leiden, the Netherlands

Global Change Biology **(2015) 21: 3074-3086.**

3.1 Abstract

Earth system models demonstrate large uncertainty in projected changes in terrestrial carbon budgets. The lack of inclusion of adaptive responses of vegetation communities to the environment has been suggested to hamper the ability of modeled vegetation to adequately respond to environmental change. In this study, variation in functional responses of vegetation has been added to an earth system model (ESM) based on ecological principles. The restriction of viable mean trait values of vegetation communities by the environment, called 'habitat filtering', is an important ecological assembly rule and allows for determination of global scale trait-environment relationships. These relationships were applied to model trait variation for different plant functional types (PFTs). For three leaf traits (specific leaf area, maximum carboxylation rate at 25 °C, and maximum electron transport rate at 25 °C) relationships with multiple environmental drivers, like precipitation, temperature, radiation and CO_2, were determined for the PFTs within the Max Planck Institute ESM. With these relationships, spatiotemporal variation in these formerly fixed traits in PFTs was modeled in global change projections (IPCC RCP8.5 scenario). Inclusion of this environment-driven trait variation resulted in a strong reduction of the global carbon sink by at least 33 % (2.1 Pg C yr^{-1}) from the 2nd quarter of the 21st century onward compared to the default model with fixed traits. In addition, the mid and high latitudes became a stronger carbon sink and the tropics a stronger carbon source, caused by trait-induced differences in productivity and relative respirational costs. These results point towards a reduction of the global carbon sink when including a more realistic representation of functional vegetation responses, implying more carbon will stay airborne, which could fuel further climate change.

3.2 Introduction

Global change projections by different earth system models (ESMs) diverge strongly in their predicted terrestrial global carbon budgets, both in the magnitude and direction of change. Differences between ESMs in projected changes in land carbon storage range from about 300 to 600 Pg carbon around 2100, depending on the climate change scenario (Jones *et al.*, 2013). One of the causes of variation among projections is that the modeled functional responses of ecosystems, e.g. the responses of vegetation productivity and autotrophic respiration to climate drivers, differ strongly among models (Sitch *et al.*, 2008). In addition, lack of inclusion of vegetation dynamics (Poulter *et al.*, 2010) and of vegetation adaptation to changing environments (Sitch *et al.*, 2008) are thought to contribute to these large inter-model deviations in global carbon budgets around 2100.

In part the limited variation in the functional responses of vegetation within most dynamic global vegetation models (DGVMs, which represent the land surface component, including vegetation dynamics, in ESMs) is caused by representing the vast range of vascular plant species by only a small number of static plant functional types (PFTs) (Van Bodegom *et al.*, 2012; Pavlick *et al.*, 2013). PFTs tend to be parameterized with a number of PFT-specific static properties, related to e.g. phenology and photosynthesis, allowing for only limited variation in vegetation behavior within PFTs. In reality, it is well known that vegetation responses to the environment are caused by environmental drivers working via multiple processes at different temporal and spatial scales, including plasticity, acclimation and (genotypic) adaptation in physiological and morphological traits (Shaw & Etterson, 2012), and, at the community scale, via shifts in species abundance and species turnover. In most current DGVMs, however, PFTs do not allow for such within-PFT dynamics, because the mechanisms underlying functional responses to environmental change are not or superficially modeled. Moreover, these functional responses of vegetation communities to environmental change also modify ecosystem functioning and the vegetation feedbacks to the environment (Lavorel & Garnier, 2002; Diaz *et al.*, 2004). Consequently, the lack of variation in traits in PFTs in most DGVMs may introduce inaccuracies in model predictions (Groenendijk *et al.*, 2011).

In response to environmental change, mean trait values of plant communities vary. Such change in traits may be determined by ecological community assembly rules, which express the impacts of 'habitat filtering' (Keddy, 1992; Cornwell *et al.*, 2006; Gotzenberger *et al.*, 2012), where the local environment constrains the viable species' trait ranges in a community. For many traits, global trait-environment relationships have already been identified (Wright *et al.*, 2005b; Ordoñez *et al.*, 2009; Douma *et al.*, 2012d; Van Ommen Kloeke *et al.*, 2012). Such relationships are used to predict community mean trait values, and thereby PFT distribution and species assemblages (Douma *et al.*, 2012a; Van Bodegom *et al.*, 2014). By using community mean traits, variation in functional vegetation responses can be modeled within PFTs based on ecological theory, but without needing to invoke mechanistic processes that are not fully quantified or understood. By quantifying the relationships between observed variation in community mean traits and their environmental drivers and incorporating these into DGVMs, traits can be adjusted every year within the model, allowing for spatial and temporal variation in functional responses of vegetation to environmental change and modification of vegetation-atmosphere feedbacks.

Equilibrium simulations based on this approach have shown very strong impacts on carbon fluxes and vegetation distribution (Verheijen *et al.*, 2013), but the impact in global change projections is unknown. Because the response of the community may be different from that expected from single species responses (Poorter & Navas, 2003) and changes in community mean trait values include both within species changes as well as changes induced by differences in species abundances, the magnitude and direction of

community-level responses and related carbon fluxes is difficult to foretell. Therefore, the aim of this study is to identify if and how the global carbon budget is modified in space and time in global change projections when multiple environmental sources of variation in functional vegetation responses are included.

We implemented trait variation within the DGVM component of the Max Planck Institute earth system model (MPI-ESM). Three leaf traits that have been static in the model so far were selected. These traits were specific leaf area (SLA, fresh leaf area per dry mass), maximum carboxylation rate at a reference temperature of 25 °C ($Vcmax_{25}$) and maximum electron transport rate at 25 °C ($Jmax_{25}$). Photosynthetic parameters are the most sensitive parameters of DGVMs (White *et al.*, 2000; Zaehle *et al.*, 2005) and varying such traits are likely to modify model performance upon global change. For these three traits, for each PFT in the model, relationships with the environment were determined. In the model these traits were reparameterized on a yearly basis depending on local environmental conditions of the previous year, allowing vegetation to respond dynamically to the environment. Projections were run separately with default static traits and variable traits, each with two simulations, one with climate and atmospheric CO_2 change and one with climate change with atmospheric CO_2 kept at pre-industrial concentrations, in order to disentangle trait impacts on modified vegetation responses and carbon fluxes with and without the inclusion of CO_2 fertilization of photosynthesis.

3.3 Materials and Methods

Model description

The MPI-ESM was developed by the Max Planck Institute for Meteorology (Germany). Fluxes of water, carbon and energy between land and atmosphere, as well as vegetation dynamics are simulated by the DGVM JSBACH (Raddatz *et al.*, 2007; Brovkin *et al.*, 2009; Reick *et al.*, 2013) which is the land surface component of the MPI-ESM. In JSBACH, grid cells are covered with different fractions of PFTs. In this setup of JSBACH, 8 PFTs were present: tropical broadleaved evergreen trees, tropical broadleaved deciduous trees, extra-tropical (both temperate and boreal) evergreen trees, extra-tropical deciduous trees, raingreen shrubs, cold/deciduous shrubs, C3-grasses and C4-grasses. Competition between woody (shrubs and trees) and non-woody classes (grasses) is based on different rates of establishment into unoccupied land. Within woody or non-woody vegetation types competition is based on multi-year net primary productivity (NPP). Mortality is natural (fractional decline) or disturbance induced (by windbreaks or fire). In this setup no anthropogenic impacts were modeled, meaning crops were not included and there was no

land use change. The setup did not include a nitrogen cycle either as this was not available for this coupled model setup at the time of the simulations.

Based on the availability of geo-referenced observational trait data, needed to determine the relationships between traits and environmental conditions, three originally PFT-specific parameters could be selected to vary: SLA ($m^2\ kg^{-1}$ carbon), $Vcmax_{25}$ (μmol $m^{-2}\ s^{-1}$) and $Jmax_{25}$ (μmol $m^{-2}\ s^{-1}$). Although in the simulation with trait variation spatial and temporal variation in these traits occurred, the functional roles of the traits remained the same as in the default simulations. For an elaborate description of these functional roles of these traits in JSBACH, see Verheijen *et al.* (2013) and its supplementary material. In short, $Vcmax_{25}$ and $Jmax_{25}$ are reference values used in the photosynthesis routine (based on Farquhar *et al.* (1980, 1988) for C3-plants and Collatz *et al.* (1992) for C4-plants) to calculate Vcmax and Jmax at ambient temperatures, and subsequently, actual carboxylation and electron transport rate. Leaf carbon assimilation (A) is then determined by the lower value of the actual carboxylation and electron transport rate, minus leaf maintenance (dark) respiration (R_d). Ambient R_d is derived from R_d at a reference temperature of 25 °C ($R_{d,25}$), which is a constant fraction of $Vcmax_{25}$.

Gross primary productivity (GPP) is obtained when A is scaled to the canopy by the leaf area index (LAI). NPP is GPP minus whole plant maintenance respiration (R_m, which scales up from leaf Rd) and growth respiration (R_g, which is a fixed portion of GPP-R_m). Within a PFT, NPP is divided in fixed fractions over different carbon pools; aboveground and belowground 'green' (resource acquisition) pools (leaves and fine roots), wood pools, reserve pools and root exudates. SLA plays no role in determining LAI, but controls, together with LAI, the maximum quantity of carbon in the green pool and the optimal quantity of carbon in the reserve pool, thus co-determining the flow of carbon to the litter pools via modification of carbon allocation dynamics. As a result, SLA is only marginally related to productivity (by determining the maximum amount of carbon that can be allocated) and is completely decoupled from phenology. As a consequence, the role of SLA on carbon fluxes is therefore limited compared to that of $Vcmax_{25}$ and $Jmax_{25}$ (see, for a more detailed discussion, Verheijen *et al.*, 2013).

The default model has been benchmarked against contemporary conditions (Brovkin *et al.*, 2013; Dalmonech & Zaehle, 2013). Verheijen *et al.* (2013) discussed the contemporary performance of the model when trait variation is included; GPP in the tropics was higher than in the default model, but it performed similarly well or better with respect to vegetation distribution and carbon pools.

Selected data and trait-environment relationships

The selected trait and climate data and the majority of the methods applied for determining the trait-environment relationships are described in detail in Verheijen *et al.* (2013).

Briefly, data for SLA, $Vcmax_{25}$ and $Jmax_{25}$ were obtained from the TRY database (Kattge *et al.*, 2011), supplemented with SLA data from Van Bodegom *et al.* (2012) and $Vcmax_{25}$ and $Jmax_{25}$ data from Domingues *et al.* (2010) (Table 1). For C4-grasses PEP-carboxylase CO_2 specificity (PEP, mmol m^{-2} s^{-1}) instead of $Jmax_{25}$ was modeled. For this PFT, PEP and $Vcmax_{25}$ data were very limited, therefore these traits were estimated based on leaf nitrogen data from the TRY database and equations from Simioni *et al.* (2004). Every trait observation was assigned to a JSBACH PFT based on information about growth form, leaf habit, photosynthetic pathway and occurrence in a climatic region of the Köppen-Geiger classification (Kottek *et al.*, 2006). Community mean trait values were calculated for each PFT, weighted by square root of the number of observations per community. For SLA, this resulted in 1052 PFT-specific entries (12394 observations over 2869 species), 70 entries for $Vcmax_{25}$ (761 observations over 129 species) and 56 entries for $Jmax_{25}$ (402 observations over 108 species).

Table 1. References of selected trait data.

Trait	**Reference**
SLA	Ackerly & Cornwell (2007); Bahn *et al.* (1999); Cavender-Bares *et al.* (2006); Cornelissen *et al.* (2003a); Cornelissen *et al.* (2004); Cornwell *et al.* (2006); Fyllas *et al.* (2009); Garnier *et al.* (2007); Kattge *et al.* (2009); Kattge *et al.* (2011); Kleyer *et al.* (2008); Kurokawa & Nakashizuka (2008); H. Kurokawa (unpublished data); Laughlin *et al.* (2010); M.R. Leishman (unpublished data); Louault *et al.* (2005); Medlyn *et al.* (1999); Niinemets (1999); Niinemets (2001); Ogaya & Peñuelas (2007); Ogaya & Peñuelas (2008); Ordoñez *et al.* (2010); Patino *et al.* (2012); Pyankov *et al.* (1999); Reich *et al.* (2008); Reich *et al.* (2009); Shipley (1995); Shipley & Vu (2002); N.A. Soudzilovskaia (unpublished data); Swaine (2007); Van Bodegom *et al.* (2012); P.M. van Bodegom (unpublished data); Vile *et al.* (2006); E. Weiher (unpublished data); Wohlfahrt *et al.* (1999); Wright *et al.* (2004); Wright *et al.* (2006b)
$Vcmax_{25}$	Domingues *et al.* (2010); Kattge *et al.* (2009); Niinemets (1999); Niinemets (2001)
$Jmax_{25}$	Domingues *et al.* (2010); Kattge *et al.* (2009)

To define trait-environment relationships, community mean trait values were related to a set of environmental drivers. For each PFT, multiple linear regression was applied to combinations of climatic variables. For CO_2 a separate regression was determined, because the response of plants to CO_2 concentrations other than ambient atmospheric CO_2 could

only be derived from CO_2 enrichment experiments. As a consequence, the established trait-environment relationships are composite regressions.

Most climate data was taken from 10 minute gridded data sets from the Climatic Research Unit (CRU) (New *et al.*, 2002), including mean annual precipitation (MAP, mm $year^{-1}$), mean annual relative humidity (Reh, %), mean annual temperature (MAT, °C), and mean temperature of coldest and warmest month (Tmin and Tmax, °C). In addition, annual soil moisture estimates (SoilMoist, m^3 m^{-3} for 1 meter depth) were taken from a 15 minute gridded data set based on remotely sensed data (Miralles *et al.*, 2011) and mean annual net shortwave radiation (NSWR, (W m^{-2}) was calculated on a 30 minute resolution following Allen *et al.* (1998) and based on CRU data on percentage sunshine.

These climatic variables were coupled to the PFT-specific trait means via geo-references. With the currently available meta-data in TRY it was not possible to link traits to the environmental conditions of the year the traits were measured. Instead, the mean of traits measured at different years was taken, assuming that they represented an 'average' year. All possible relationships were tested by multiple linear regression (including interactions). After checking for significance and co-linearity of the environmental drivers and residual distribution, regressions with the highest $R^2_{adjusted}$ were selected. Due to the low number of entries for the two tropical tree PFTs and the two shrub PFTs, data were combined, resulting in two instead of four regressions for these PFTs. To prevent modeling unrealistic trait values, simulated traits were restrained to a 2.5-97.5% species-level quantile interval. Given that $Vcmax_{25}$ and $Jmax_{25}$ are strongly correlated (Wullschleger, 1993), PFT-specific confidence intervals for their relationship were applied as an additional constraint.

In contrast to plant responses to climate, which could be based on field data, the response of plants to elevated CO_2 concentrations could only be determined experimentally. For this, we used meta-analyses of CO_2 enrichment experiments. Due to the relatively sparse data, some PFTs were grouped. For trees, the elevated CO_2 responses of $Vcmax_{25}$ and $Jmax_{25}$ were derived from the meta-analysis of Medlyn *et al.* (1999), and for shrubs and C3-grasses from Ainsworth & Rogers (2007). C4-grasses did not show a significant response. For SLA, responses from Poorter *et al.* (2009) were taken for C3-plants (woody and non-woody plants) and C4-plants. Elevated CO_2 concentrations were approximately 700 ppm in Medlyn *et al.* (1999), on average 567 ppm in Ainsworth & Rogers (2007) and up to 1000 ppm in Poorter *et al.* (2009).

For C3-plants, the responses of PFTs to elevated CO_2 resulted in a decrease in trait values. For $Vcmax_{25}$, this reflects a down-regulation upon increasing CO_2, caused by an increased affinity of Rubisco for CO_2 at the expense of O_2 affinity at higher internal CO_2 concentrations (Leakey *et al.*, 2012). In addition, there is less ATP needed for RuBP regeneration, allowing a reduction in $Jmax_{25}$ as well. Longer-term reduction in $Vcmax_{25}$ is associated with a reduction in leaf nitrogen, which is re-allocated to other plant components

to optimize carbon gain and resource use, especially within an nitrogen-limited environment (Ainsworth & Rogers, 2005; Leakey *et al.*, 2012). In addition, longer-term down-regulation of photosynthesis is also associated with an increase in non-structural carbohydrates like starch (Poorter *et al.*, 2009; Leakey *et al.*, 2012), explaining why SLA might decrease with increasing CO_2 in C3-plants. In contrast, in C4-grasses no change in SLA was found, the causes of which remain unclear (Poorter *et al.*, 2009). $Vcmax_{25}$ and PEP did not show a strong response in C4-grasses, because these grasses have a CO_2-concentrating mechanism leading to CO_2 saturation rather independent from atmospheric CO_2 concentrations (Poorter & Navas, 2003). However, they can still benefit from higher atmospheric CO_2 by an increased water use efficiency via reduced stomatal conductance (Ainsworth & Rogers, 2007).

The different regressions for CO_2 and the climatic variables were combined (see S1 for a description of the regressions) and implemented in JSBACH. Trait values were calculated at the beginning of each simulated year, to allow simulation of trait values for the coming year based on the mean annual environmental conditions of the previous year for each PFT in each grid cell.

Experimental design

Four simulation experiments were carried out: two simulations with the default setup with the original default fixed trait values (DEF), and two including environment-driven variation in traits (VARTR). For each setup, one simulation with climate and atmospheric CO_2 changes was run, allowing for CO_2 fertilization effects on photosynthesis (called +fert), and one simulation with climate change but without CO_2 fertilization (called -fert), by keeping atmospheric CO_2 fixed at pre-industrial concentrations (atmospheric CO_2 set at 284.7 ppm, approx. year 1850). In contrast to the DEF simulations, in both VARTR simulations environmental change played an additional role in varying traits, although in VARTR-fert, the effect of CO_2 on traits in VARTR-fert was constant over the years because CO_2 was kept constant. With these simulations, interactions between trait variation and climate change (-fert) and the combined effects of both climate change and CO_2 fertilization (+fert) on carbon fluxes could be investigated.

Simulations were performed with the MPI-ESM at a land resolution of 1.875° (T63). Climate was internally simulated by the atmosphere model ECHAM6 (Stevens *et al.*, 2013) and fluxes between land and atmosphere and vegetation dynamics by JSBACH. Seasonal sea surface temperatures and sea ice were prescribed and taken from simulations by fully coupled historical runs (1850-2004) and projections (2004-2100) from the C5MIP model intercomparison project following the RCP8.5 scenario (Van Vuuren *et al.*, 2011). The same input of ozone, aerosols and radiative forcing as in the C5MIP project were used, see Giorgetta *et al.* (2013) for an overview and description of sources. Only natural

vegetation was modeled, and therefore anthropogenic greenhouse gas emissions (CO_2, N_2O, CH_4 en CFCs) were prescribed, following the RCP8.5 scenario as well, which implies a steady increase in atmospheric CO_2 to 925.9 ppm around 2100. The consequence of this prescribed atmospheric CO_2 increase was that carbon feedbacks were not accounted for in the model.

Default simulations and simulations with variation in traits in PFTs had their own model initialization. For each model setup, the coupled JSBACH/ECHAM5 model was run until quasi-equilibrium (for the vegetation) for 250 years in the pre-industrial climate by repeating 30 years of seasonal sea surface temperatures and sea ice forcing and running vegetation dynamics in an accelerated mode (where vegetation responses were simulated 3 times within each year). The last 30 years of this spin-up were used to drive the carbon balance model of JSBACH for 1500 years to get the soil carbon pools into equilibrium. Then the model was restarted with the equilibrated carbon pools and run for another 200 years (with vegetation dynamics in a normal mode) to get vegetation in equilibrium. The two different spin-ups were used to start the historical run and projections of the +fert and -fert simulations (i.e. DEF+fert and DEF-fert and VARTR+fert and VARTR-fert). This means the DEF and VARTR simulations had different initial climate and vegetation properties and carbon stocks, but +fert and -fert for either the DEF or the VARTR setup did not.

Simulations were performed till 2100 with CO_2 concentrations increasing up to ~925 ppm. For SLA, these concentrations fell within the calibration range of the meta-analysis, but maximum CO_2 concentrations in the meta-analyses used to determine $Vcmax_{25}$ and $Jmax_{25}$ responses to CO_2 were on average lower. As a consequence, CO_2 concentrations were outside the calibration range for grasses and shrubs for these traits from 2055 onward (i.e. above 567 ppm) and for trees from about 2073 onward (700 ppm). This means that results should be interpreted with care from 2055 onward, and especially the last quarter of the century should be considered speculative.

3.4 Results

Contemporary estimates of carbon budgets

The land carbon exchange, or net ecosystem exchange (NEE), of the variable traits simulation with both climate change and CO_2 fertilization effects (VARTR+fert) predicted a land carbon uptake in the 1980s, 1990s and 2000s (Table 2, positive values mean land carbon uptake). These predictions fell within the 90 % confidence interval of the global land carbon budget of the 1990s and 2000s, as estimated by the IPCC 2013 assessment (Ciais *et al.*, 2013), whereas the default simulation (DEF+fert) only fell within the 1990s

range. VARTR+fert had a lower NEE and was closer to the mean estimate than DEF+fert for either the 1980s, 1990s or 2000s. Either simulation with climate change but without CO_2 fertilization effects (DEF-fert and VARTR-fert) predicted a land carbon release for each of the contemporary time periods.

Projected global NEE

Both simulations with climate change and CO_2 fertilization effects (DEF+fert and VARTR+fert) showed an increase in land carbon initially (Fig. 1), but NEE started to level off towards 2050 and showed a steadily decline in NEE in the second half of the 21st century. Compared to the DEF+fert simulation, land in the VARTR+fert simulation was a weaker carbon sink (see also carbon pools in Fig. S2). Projected NEE was on average 2.1 Pg C yr^{-1} lower in the 2nd and 3rd quarters of the 21st century, and 2.7 Pg C yr^{-1} lower in the last quarter, which means respectively 33.0, 36.2 and 69.9 % less carbon sequestration in VARTR+fert than in DEF+fert in these periods.

Table 2. Comparison of simulated global land carbon budgets (positive values mean land carbon uptake) with the estimates from the IPCC 2013 report (Ciais et al., 2013). Carbon in Pg C yr^{-1}, in brackets the 90 % confidence interval.

	1980s *Pg C yr $^{-1}$*	1990s *Pg C yr $^{-1}$*	2000s *Pg C yr $^{-1}$*
IPCC 2013 Residual Land Sink	1.5 (0.4 - 2.6)	2.6 (1.4 - 3.8)	2.6 (1.4 - 3.8)
DEF+fert	3.05	3.21	3.98
VARTR +fert	2.89	2.4	3.49
DEF-fert	-0.94	-0.55	-1.29
VARTR-fert	-0.43	-1.11	-1.00

In the -fert simulations (DEF-fert and VARTR-fert), the lack of CO_2 fertilization on photosynthesis resulted in a steady weakening of the land carbon sink over time, because the increase in both autotrophic (Ra) and heterotrophic (Rh) respiration due to higher temperatures was not compensated by an increase in GPP, like in the +fert simulations (see Fig. S3 for separate fluxes). Land in the VARTR-fert was a stronger carbon source than in DEF-fert, although differences were smaller than between +fert simulations. NEE in VARTR-fert was 0.3 Pg C yr^{-1} lower (more negative) in the 2nd quarter, and 1.0 Pg C yr^{-1} lower in both the 3rd and 4th quarter of the 21st century, which represented an increase in the carbon source of 11.1, 28.8 and 21.7 % , respectively, compared to DEF-fert.

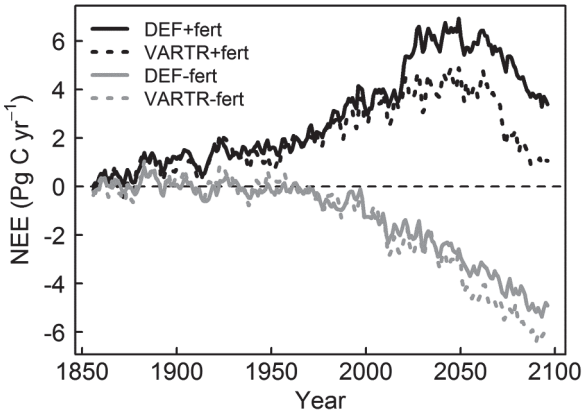

Figure 1. Global net ecosystem exchange (10-year running mean in Pg C yr^{-1}). Positive values mean land carbon uptake.

In VARTR, NEE differences between the (combined) effects of CO_2 fertilization (+fert) and climate change versus climate change alone (-fert) were 1.8, 1.0 and 1.7 Pg C yr^{-1} less in the last 3 quarters of the 21st century compared to differences between +fert and -fert in DEF. This means that by including trait variation, the (combined) effects of CO_2 fertilization and climate change on the global carbon sink and source patterns were modified as well.

Latitudinal changes in NEE

Latitudinal NEE (Fig. 2) clarifies which areas contributed most to the changes in global NEE. For the contemporary climate, differences across latitudes and among simulations were small. However, over time, differences in latitudinal NEE between simulations became more profound, both in the amount of carbon sequestered or released and in the spatial distribution. In addition, global variability in NEE increased over time and was larger in VARTR than in DEF simulations (compare standard deviations in Fig. 2). From around 2050, NEE of the tropics (defined as area between the Tropic of Cancer and Tropic of Capricorn) started to diverge more strongly from NEE at the mid and high latitudes (i.e. temperate, boreal and arctic areas in the northern hemisphere) in VARTR simulations compared to the DEF simulations. This divergence was caused both by a stronger increase in carbon sequestration in the mid and high latitudes and a stronger carbon release in the tropical areas in the VARTR simulations.

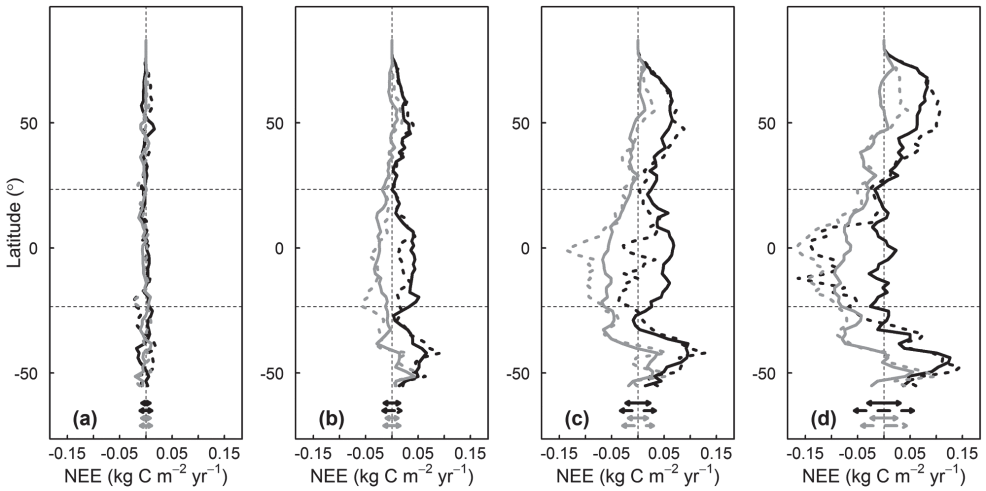

Figure 2. Latitudinal gradients of (10-year mean) average net ecosystem exchange (kg C m^{-2} yr^{-1}**),** with global standard deviations (bottom horizontal lines): a) 1851, b) 2000, c) 2050, d) 2100. Legend as in Fig. 1. Horizontal dashed lines denote the Tropic of Cancer and Capricorn.

Latitudinal changes in traits

In general, latitudinal gradients of mean trait values averaged over all PFTs (and weighted by fractional cover of a PFT in a grid cell) showed a decreasing trend over time in VARTR+fert (Fig. 3), but in VARTR-fert, traits changed less and even increased in some areas (e.g. above 50°N). In contrast, in both DEF simulations shifts in traits were small, because weighted mean trait values in grid cells could only change with shifts in PFT cover. In all simulations, $Vcmax_{25}$ and $Jmax_{25}$ were clearly lower in the tropics than at mid and high latitudes, due to more favorable environmental conditions (e.g. higher temperatures and a longer growing season).

Variation in traits was induced by both changes in climatic drivers and CO_2 in VARTR+fert. By removing the CO_2-induced variation from the VARTR+fert trait values, trait changes over time (left to right panels) caused by climatic variables alone (blue line in Fig. 3) could be investigated. In addition, the difference between trait values based on all environmental drivers (black dashed line) and climatic drivers alone (blue line) reflects the amount of change induced by elevated CO_2.

Climate-induced variation in PFT-averaged trait values resulted in trait patterns of VARTR+fert shifting strongly towards those of VARTR-fert (i.e. blue lines and grey dashed lines), where CO_2 did not affect vegetation and traits thus varied in response to climate only. Trait values, however, did not completely overlap, reflecting trait-induced differences in climate and vegetation cover among the VARTR simulations. These climate-

induced changes could both increase or decrease over time, depending on the dominant PFT (see also Fig. S4 for PFT-specific trait responses over time). In contrast, including the response of CO_2 always resulted in a decrease in trait values (expect for SLA for C4-grasses). The net changes in traits depended on both the amount and direction of change induced by both climatic variables and CO_2, which varied between PFTs (Fig. S4). The relative contribution of CO_2 and climate to variation in traits was therefore also PFT-dependent.

Latitudinal changes in fluxes

In the DEF+fert simulation, GPP steadily increased over time in mid and high latitudes as well as the tropics, whereas in VARTR+fert, GPP started already to decline in the equatorial tropics in the 2nd quarter of the 21st century. Changes in traits affected GPP, but productivity in the +fert simulations was mostly determined by direct CO_2 fertilization effects, because GPP still increased even when $Vcmax_{25}$ and $Jmax_{25}$ decreased (compare Fig. 3 and Fig. 4). In most cases, when $Vcmax_{25}$ and $Jmax_{25}$ dropped below values as prevailing in DEF+fert, this resulted in a lower GPP in VARTR+fert as well.

Overall, the NPP:GPP ratio (Fig. 5) was lower for all simulations in the tropics compared to the high latitudes, because higher temperatures enhances respiration in the tropics (Raddatz *et al.*, 2007). Changes in this ratio were caused by direct CO_2 fertilization effects and temperature effects on GPP and temperature effects on Ra. Changes in $Vcmax_{25}$ and $Jmax_{25}$ modified this ratio additionally, making it difficult to disentangle the relative contribution of each variable. Over time, the areas in the mid and high latitudes where the NPP:GPP ratio was higher in VARTR+fert than in DEF+fert increased over time, indicating relatively lower respirational costs in VARTR+fert. Even though GPP was equal to or lower than in DEF+fert, this resulted in higher NEE in large parts of these regions from around 2050 onward in VARTR+fert. In contrast, in the tropics, the NPP:GPP ratio was almost always lower (meaning relatively higher respirational losses) in VARTR+fert, independent of whether GPP was lower or higher than in DEF+fert. Over time, Rh became slightly lower (Fig. S5) in VARTR+fert, but this could not compensate for the lower carbon use efficiency, and NEE dropped to negative values around 2050.

In the -fert simulations, these dynamics of fluxes and traits resulted in similar differences: a somewhat higher NEE for VARTR-fert at higher latitudes, and lower NEE in the tropics compared to DEF-fert.

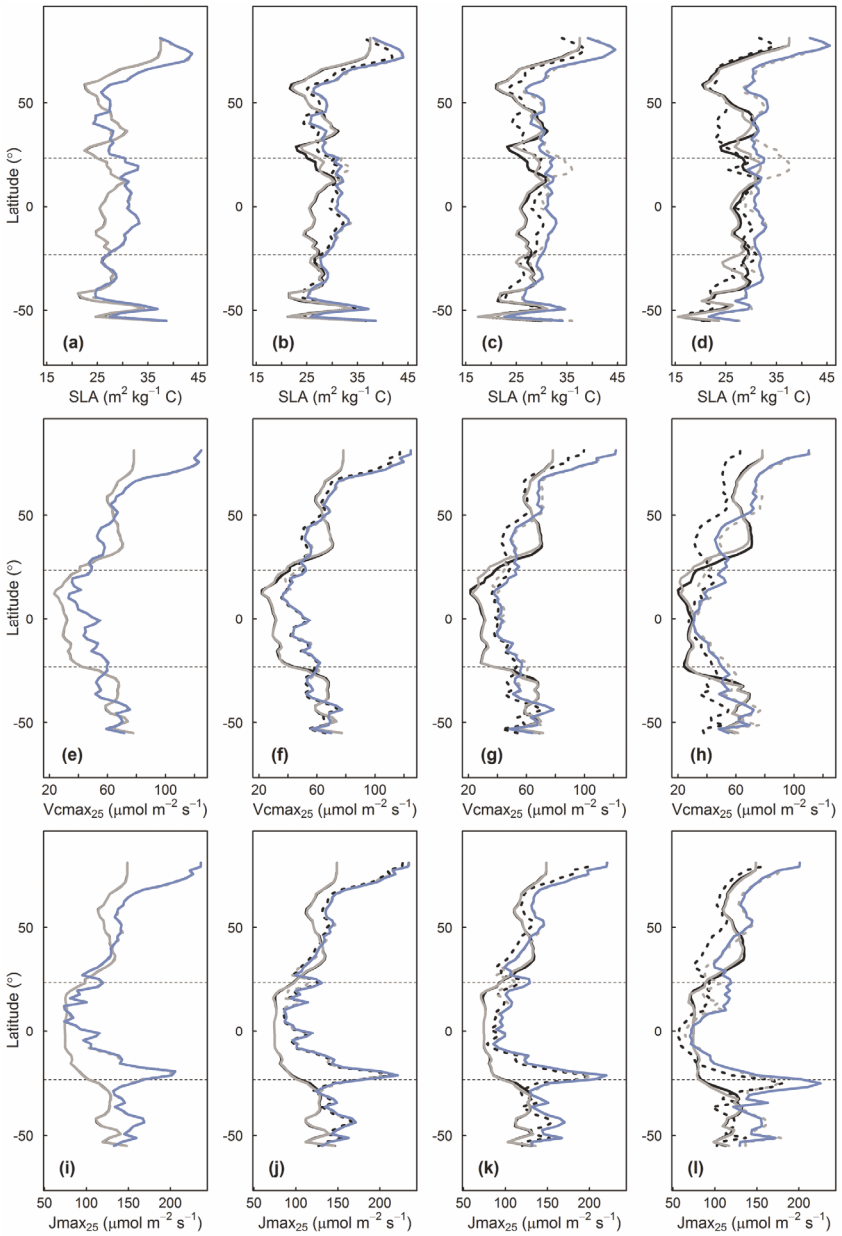

Figure 3. Latitudinal gradients of (10-year mean) trait values, weighted by fractional PFT cover: a (a, e, i) 1851, (b,f,j) 2000, (c,g,k) 2050, and (d,h,l) 2100. Upper row, SLA (kg m^{-2}), middle row $Vcmax_{25}$ (µmol m^{-2} s^{-1}), lower row $Jmax_{25}$ (µmol m^{-2} s^{-1}, without C4-grasses). Legend as in Fig. 1. In addition, blue line: VARTR+fert without CO_2 response. Horizontal dashed lines denote the Tropic of Cancer and Capricorn. Note that in 1851 trait values within DEF and VARTR overlap initially and therefore some simulations seem absent.

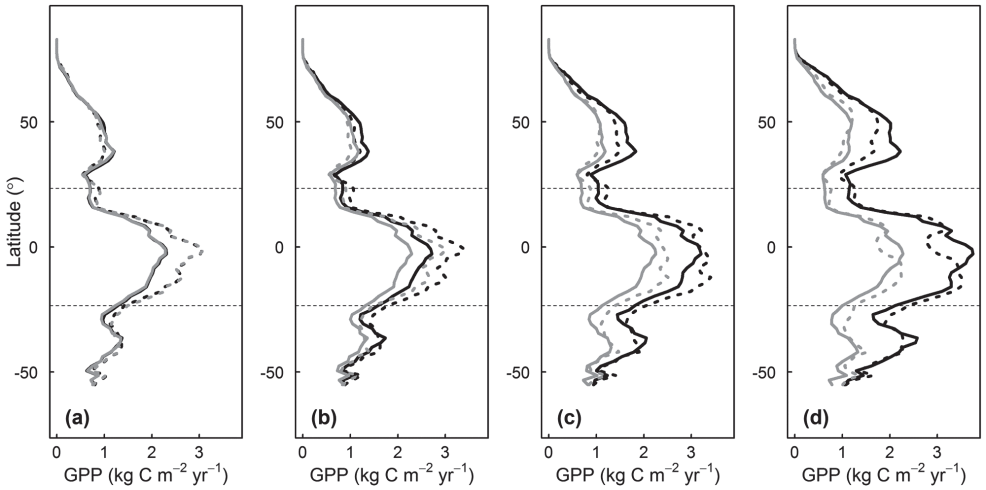

Figure 4. Latitudinal gradients of (10-year mean) average annual GPP (kg C m^{-2} yr^{-1}): a) 1851, b) 2000, c) 2050, d) 2100. Legend as in Fig. 1. Horizontal dashed lines denote the Tropic of Cancer and Capricorn.

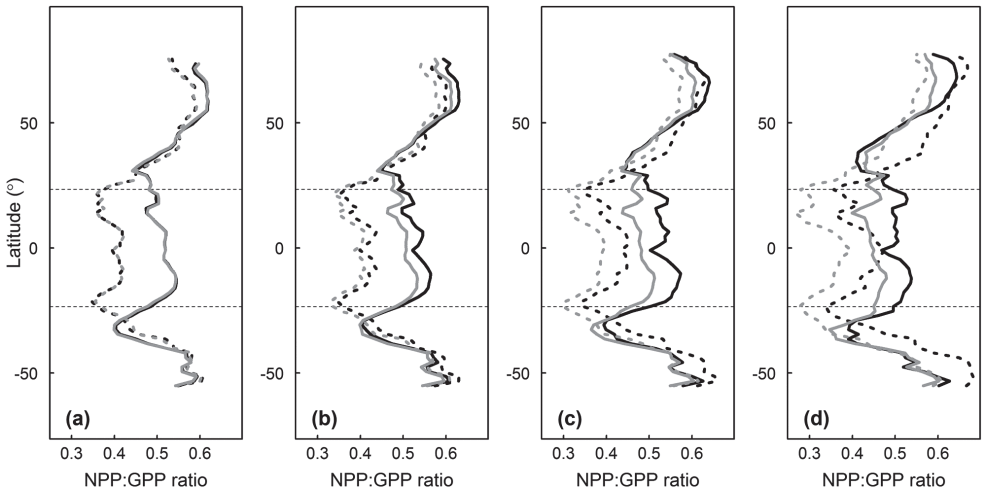

Figure 5. Latitudinal gradients of (10-year mean) NPP:GPP-ratios: a) 1851, b) 2000, c) 2050, d) 2100. To prevent numeric artefacts, areas where GPP is≤0.05 are left out. Legend as in Fig. 1. Horizontal dashed lines denote the Tropic of Cancer and Capricorn.

3.5 Discussion

Implications of trait variation for global and regional responses in carbon fluxes

In this study, we implemented trait variation within PFTs based on observed trait-environment relationships, allowing for variation in functional responses to changes in the environment within PFTs. This approach is a logical next step from using PFTs with static properties, which hampers the modeling of more dynamic functional vegetation responses (Kattge *et al.*, 2011; Van Bodegom *et al.*, 2012; Pavlick *et al.*, 2013). Allowing for a more realistic functional response of vegetation to environmental change by including trait variation allowed for better estimates of contemporary global land carbon uptake (Table 2), and altered global and regional source-sink patterns of carbon.

Even though the direct CO_2 fertilization effect on GPP was more profound than the effect of trait variation on GPP (compare the change over time in GPP in VARTR+fert and VARTR-fert simulations), changes in traits modified GPP and affected NEE. This resulted in a lower NEE in VARTR+fert compared to DEF+fert of on average 2.1 Pg C yr^{-1} between 2026 and 2075 and about 2.7 Pg C yr^{-1} in the final quarter of the 21st century, although this last projection remains rather uncertain due to extrapolation of trait responses to elevation CO_2 beyond the calibration range. Regionally, however, NEE also increased, particularly at the mid and high latitudes. The strong reduction in NEE in VARTR+fert can mostly be attributed to the tropics, where predictions are relatively uncertain, as data availability for the calibration of trait-environment relationships was limited (see Materials and Methods section). The robustness of this outcome thus needs to be evaluated in future studies.

The actual effects of traits on model performance are difficult to pinpoint due to the different pathways by which variation in traits can cascade trough the model. Changes in traits drive changes in GPP ($Vcmax_{25}$ and $Jmax_{25}$), Ra ($Vcmax_{25}$, via $R_{d,25}$) and carbon storage (SLA), and consequently modify carbon use efficiency via the NPP:GPP ratio. Moreover, the effects of changes in traits do not only work via modification in vegetation carbon fluxes, but also indirectly through effects on vegetation distribution (via NPP-induced shifts in competitive advantage), Rh (via litter quality and quantity) and feedbacks to climate (e.g. via changes in productivity or vegetation distribution, see Verheijen *et al.* 2013). These multiple pathways via which trait effects the carbon cycle can cascade through the system, is probably the main cause for the modification of functional vegetation responses by variable traits to be strongly region dependent.

In addition, trait effects on vegetation and fluxes are not easy to disentangle from direct effects of changes in climate or CO_2 fertilization effects. However, by comparing differences between DEF+fert and DEF-fert with differences between VARTR+fert and

VARTR-fert, it was possible to identify to which extent trait variation affected the (combined) effects of climate change and CO_2 fertilization (+fert simulations) on global carbon sequestration compared to climate change effects alone (-fert simulations). Globally, this effect of variable traits (comparing +fert to -fert simulations) was substantial and dampened global carbon sequestration by on average 1.8 Pg C yr^{-1} in the 2nd quarter and 1.0 Pg C yr^{-1} and 1.7 Pg C yr^{-1} in the 3rd and 4th quarter of the 21st century in VARTR compared to DEF. While the relative contribution of CO_2 and climatic variables to variation in traits differed per PFT, CO_2-induced trait responses consistently resulted in a decrease in global PFT-averaged trait values. Especially for $Vcmax_{25}$ and $Jmax_{25}$, this resulted in lower trait values and productivity, dampening the effect of CO_2 fertilization on photosynthesis and resulting in smaller differences between +fert and -fert in VARTR than in DEF.

Together, these results suggest that our model, but potentially other ESMs as well, currently overestimates projected land carbon uptake, which implies more CO_2 than expected will stay airborne at the end of the 21st century.

Challenges for including trait variation in DGVMs

Due to gaps in current knowledge and available data, some uncertainties concerning the trait-environment relationships as applied in the current approach remain to be resolved. For some PFTs the number of trait data was limited, and in some cases the fraction of trait variance explained by environmental drivers was low (see S1). However, the established trait-environment relationships are based on community mean traits and thus less prone to biases caused by large differences in the number of observations for individual species.

In addition, the incorporated relationships are based on spatial patterns in trait-environment relations and subsequently applied to predict future temporal patterns in trait variation. The applicability of such relationships under future climate is uncertain, because i. acclimation and adaptation processes may affect trait-environment relationships, ii. prevailing vegetation may lag in its response (Chapin & Starfield, 1997) or may not respond in similar ways to imposed environmental changes as the responses inferred from community mean trait-environment relationships, and iii. the combination of future climate, atmospheric chemistry and soil properties may lead to novel abiotic regimes and ecosystem types that cannot easily be predicted from knowledge about the present or past (Chapin & Starfield, 1997; Reu *et al.*, 2014).

Concerning the first point, the importance of and variation in trait acclimation and adaptation to environmental change are currently largely unknown at a global scale and can therefore not yet be quantitatively incorporated in DGVMs. For example, long-term temperature and CO_2 acclimation of photosynthesis and temperature acclimation of respiration is lacking in most global models (Smith & Dukes, 2013). In our model, vegetation acclimation and adaptation to elevated CO_2 are based on measured PFT-specific

responses, but measurements on vegetation responses to long-term CO_2 enrichment treatments with very high concentrations of CO_2 are still relatively scarce. Trait responses to environmental changes might be modified by interactions between CO_2 and other environmental drivers, whereas our trait-environment regression are composite additive regressions. However, long-term studies (spanning several growing seasons) investigating such interactions on plant performance are still limited, and interactions do not always occur (as e.g. between CO_2, temperature and drought, Kongstad *et al.*, 2012; Arndal *et al.*, 2014) or show idiosyncratic responses (e.g. for the interactive effect between CO_2 and nitrogen, see Norby & Zak (2011) for an overview). In addition, trait responses to CO_2 are very likely to change with increasing atmospheric CO_2, because these trait changes do not stand alone from other physiological processes, like reductions in stomatal conductance, nitrogen re-allocation and accumulation of sugars (Leakey *et al.*, 2012), all of which can modulate the response of $Vcmax_{25}$ and $Jmax_{25}$ to CO_2. Due to data limitations, however, a more sophisticated modeling of the actual responses of these traits beyond assuming a linear response was currently out of reach. Because of these uncertainties in adaptive and interactive responses, results after 2050 need to be interpreted with care, also because $Vcmax_{25}$ and $Jmax_{25}$ responses to CO_2 concentrations are outside the range of the meta-analysis for shrubs and grasses from 2055 onward (i.e. above 567 ppm), even though for trees these responses are still within the calibration range till about 2073 and SLA responses can be extrapolated to the end of the century.

With respect to the second uncertainty, it appears that the observed intra- and interannual variation in LMA (leaf mass per area, inverse of SLA) of oaks and perennial grasses (6 year time span) (Ma *et al.*, 2011) and $Vcmax_{25}$ in oak and ash (3 year time span) (Grassi *et al.*, 2005) is as strong as the simulated variation in the traits of deciduous trees or C3-grasses over a period of 250 years. This demonstrates the huge amount of variation in leaf traits possible within only a few years and shows the responsiveness of vegetation to changing environmental conditions. Moreover, over a 250 year time period (the length of the simulations), variation in functional vegetation responses of non-woody vegetation (in much lesser amount in woody vegetation due to longer turn-over times) might additionally be driven by genetic adaptation or shifts in species abundance. Thus, although the use of trait-environmental relationships has its limitations for applications in global modeling, its inclusion allows accounting for variation in traits within PFTs within realistic ranges, which have been shown to be very large.

Concerning the last point, moving away from PFTs towards a completely traits-based modeling approach can allow for non-analogue vegetation types (Van Bodegom *et al.*, 2012; Reu *et al.*, 2014). In our model, we set additional limits on traits to prevent unrealistic trait ranges outside observed ranges. Therefore, we may have conservatively assessed the impacts of potential no-analogue conditions.

In addition to these uncertainties concerning data availability and knowledge gaps about vegetation responses, the model design also poses limitations on the implementation of trait variation. Plant traits are often correlated, and we accounted for such trade-offs for $Vcmax_{25}$ and $Jmax_{25}$. However, well known trade-offs from the 'leaf economics spectrum' (Wright *et al.*, 2004), e.g. between SLA and these photosynthetic traits or leaf life span (LLS), could not be implemented because in JSBACH phenology is modeled independently from productivity and carbon storage. Hence, in contrast to many DGVMs, in JSBACH SLA is not linking productivity and leaf area index (LAI). This decoupling of SLA makes trade-offs with photosynthetic traits and LLS less relevant, although in other vegetation models with a more central role for SLA, such trade-offs are necessary. For a more elaborate discussion on this, we refer to Verheijen *et al.* (2013).

Towards a more realistic vegetation representation by including an integrated estimate of trait variation

A number of alternative approaches have been developed to realize more (trait) variation in vegetation models, from realizing trait variation as an emergent property based on fundamental trade-offs (Pavlick *et al.*, 2013; Scheiter *et al.*, 2013) to data-driven approaches based on observed species trait values (Fyllas *et al.*, 2014). So far, none of these approaches use integrated estimates of community-level trait variation by linking observational trait data to multiple environmental drivers. Community mean trait responses include both within-species acclimation or adaptation as well as changes in trait values caused by shifts in species abundances as a consequence of competition or environment-induced mortality. Both components need to be considered given that single species responses do not necessarily translate to responses at the community-level (Poorter & Navas, 2003). Moreover, the combination of responses also implies that trait responses will not automatically result in biomass increment in a community. For example, at the end of the 21st century, there was a drop in the productivity of tropical forests in the VARTR+fert simulation, whereas GPP kept increasing in DEF+fert. This makes it very difficult to predict the direction of change in carbon fluxes a priori.

In addition, by empirically including multiple environmental drivers various sources of trait variation were captured. Due to model limitations, edaphic drivers, such as nitrogen and phosphorus availability or soil age and structure are still lacking. Indirectly though, at least nutrient limitation is partially covered by the inclusion of vegetation responses to elevated CO_2, because nutrient limitation may arise when vegetation is exposed to higher CO_2 for longer time periods (Reich *et al.*, 2006; Norby *et al.*, 2010). This means that in the VARTR+fert simulation predictions are more conservative than in the DEF simulation (without any nutrients constraints at all), in results are in line with

JSBACH simulations with N and P cycling, where projected land carbon uptake is reduced due to lower productivity caused by nutrient limitations (Goll *et al.*, 2012).

Together, with our approach, a more realistic response of vegetation to changing environmental conditions, by allowing for both spatial and temporal trait variation within PFTs, can be implemented in ESMs. To further study these responses, we propose i. further development of trait databases to improve the reliability of the vegetation responses to changing climate, ii. inclusion of our approach within other DGVMs, and iii. further development of completely traits-based DGVMs. In our case, an integral assessment of these modifications in the carbon cycle through functional vegetation responses has already revealed substantial impacts on global and regional fluxes.

3.6 Acknowledgment

This study has been financed by the Netherlands Organization for Scientific Research (NWO), Theme Sustainable Earth Research (project number TKS09-03). The authors are grateful to the TRY initiative on plant traits (http://www.try-db.org). TRY is hosted, developed and maintained at the Max Planck Institute for Biogeochemistry, Jena, Germany, and is or has been supported by DIVERSITAS, IGBP, the Global Land Project, QUEST and GIS 'Climat, Environnement et Société' France. Finally, the authors thank Veronika Gayler (Max Planck Institute for Meteorology, Hamburg, Germany) for the technical and methodological support on the projections and Marjan van de Weg (Abertay University, Dundee, United Kingdom) for her help on interpreting $Vcmax_{25}$ responses.

3.7 Supplementary material

S1 Description of trait-environment relationships

Below, the derived PFT-specific equations to calculate traits as used in VARTR+fert and VARTR-fert are given, see also table 2 in Verheijen *et al.*, (2013).

Abbreviation and units are similar as in the main paper, except for:
- SLA in m^2 mol $carbon^{-1}$, in main paper this was converted to m^2 kg^{-1} dry weight.
-Net shortwave radiation in (MJ m^{-2} day^{-1}), converted from JSBACH units (Watt m^{-2}) by 0.086400.

PFT 1: Tropical evergreen trees
SLA = 1.029 + (-0.000240*MAP) + (-0.0572*NSWR) + (0.0000187*MAP*NSWR)
n= 69, R^2_{adj} = 0.092
$Vcmax_{25}$ = -1444.077 + (55.225*MAT) + (1.055* MAP) + (-0.0393*MAT*MAP)
n=9, R^2_{adj} = 0.83
$Jmax_{25}$ = -2121.955 + (80.374*MAT) + (1.514*MAP) + (-0.0555*MAT*MAP)
n=9, R^2_{adj} = 0.68

PFT 2: Tropical deciduous trees
SLA = 0.324 + (-0.0193*Tmin) + (-0.0000622*MAP) + (0.00774*Reh)
n= 38, R^2_{adj} = 0.30
$Vcmax_{25}$ = -1444.077 + (55.225*MAT) + (1.055*MAP) + (-0.0393*MAT*MAP)
n=9, R^2_{adj} = 0.83
$Jmax_{25}$ = -2121.955 + (80.374*MAT + (1.514* MAP) + (-0.0555*MAT* MAP)
n=9, R^2_{adj} = 0.68

PFT 3: extra-tropical evergreen trees
SLA = 0.0967 + (0.00588*MAT) + (0.0000516*MAP) + (-0.00615*NSWR)
n=363, R^2_{adj} = 0.29
$Vcmax_{25}$ = -244.424 + (7.407*MAT) + (-0.0802*MAP) + (4.170*Reh)
n=15, R^2_{adj} = 0.28
$Jmax_{25}$ = 294.028 + (4.414*Tmin) + (-0.141*MAP) (n=12, R^2 = 0.28)
n=12, R^2_{adj} = 0.28

PFT 4: extra-tropical deciduous trees
SLA=1.756 + (-0.0887*Tmax) + (-0.0188*Reh) + (0.00124*Tmax*Reh)
n=177, R^2_{adj} = 0.056

$Vcmax_{25}$ = 700.719 + (-8.030*Reh) + (-288.466*SoilMoist) + (28.753*Reh*SoilMoist)
n=19, R^2_{adj} = 0.34

For $Jmax_{25}$ two regressions are used, as the best model covered a relatively small environmental range. Therefore, an additional regression model was applied to these areas that fell outside the environmental range of the first model.

*If Tmin between -12.6 and 5.8 °C and NSWR between 6.814 and 12.621 MJ*m^{-2}*day^{-1}, then:*
$Jmax_{25}$ = -146.868 + (75.223*Tmin) + (25.737*NSWR) + (-7.046*Tmin*NSWR)
n=10, R^2_{adj} = 0.71

In other environmental conditions:
$Jmax_{25}$ = 446.347 + (-0.305*MAP) + (-1280.787*SoilMoist) + (1.237*SoilMoist* MAP)
n=10, R^2_{adj} = 0.44

PFT 5: raingreen shrubs
SLA = 0.848 + (-0.000350*MAP) + (-0.0532*NSWR) + (0.0000362*MAP*NSWR)
n=178, R^2_{adj} = 0.26
$Vcmax_{25}$ = 177.011 + (-0.131*MAP) + (-1.851*Reh) + (0.00192*MAP*Reh)
n=15, R^2_{adj} = 0.45
$Jmax_{25}$ = 224.822 + (0.0313*MAP) + (-504.669*SoilMoist)
n=13, R^2_{adj} = 0.64

PFT 6: cold/deciduous shrubs
SLA = 0.379 + (0.00798*MAT)
n=39, R^2_{adj} = 0.13
$Vcmax_{25}$ = 177.011 + (-0.131*MAP) + (-1.851*Reh) + (0.00192*MAP*Reh)
n=15, R^2_{adj} = 0.45
$Jmax_{25}$ = 224.822 + (0.0313*MAP) + (-504.669*SoilMoist)
n=13, R^2_{adj} = 0.64

PFT 7: C3-grasses
SLA=-0.272+(0.0119*Tmax + (0.00768*Reh)
n=153, R^2_{adj} = 0.12
$Vcmax_{25}$ = 77.403 + (-2.582*MAT)
n=4, R^2_{adj} = 37
$Jmax_{25}$ = 146.305 + (-4.686*MAT)
n=4, R^2_{adj} = 0.63

PFT 8: C4-grasses
SLA = 1.188 + (-0.0590*NSWR)
n=35, R^2_{adj} = 0.40
$Vcmax_{25}$ = -2.924 + (2.416*NSWR)
n=8, R^2_{adj} = 0.51
PEP = -281.258 + (36.618*NSWR)
n=8, R^2_{adj} = 0.51

CO_2 response terms
Final trait values in VARTR were calculated by adding an additional CO_2 response term to trait values derived from above described regressions (below referred to as $SLA_{,clim}$, $Vcmax_{25,clim}$, and $Jmax_{25,clim}$). The reference concentration ($CO_{2,ref}$) was 353.9 ppm and the elevated CO_2 concentration ($CO_{2,elev}$) was given by the model.

$Vcmax_{25}$ and $Jmax_{25}$
The CO_2 acclimation for trees was based on Medlyn *et al.* (1999).
Trees:
$Vcmax_{25} = (-0.000257*CO_{2,elev}+1.090) / (-0.000257*CO_{2,ref}+1.090) * Vcmax_{25,clim}$
$Jmax_{25} = (-0.000343*CO_{2,elev}+1.120) / (-0.000343* CO_{2,ref}+1.120) * Jmax_{25,clim}$

The CO_2 acclimation for grasses and shrubs was based on Ainsworth & Rogers (2007).
Grasses:
$Vcmax_{25} = (-0.000757*CO_{2,elev}+1.274) / (-0.000757*CO_{2,ref}+1.274) * Vcmax_{25,clim}$
$Jmax_{25} = (-0.000380*CO_{2,elev}+1.138) / (-0.000380*CO_{2,ref}+1.138) * Jmax_{25,clim}$

Shrubs:
$Vcmax_{25} = (-0.000649*CO_{2,elev}+1.236) / (-0.000649*CO_{2,ref}+1.236) * Vcmax_{25,clim}$
$Jmax_{25} = (-0.000707*CO_{2,elev}+1.257) / (-0.000707*CO_{2,ref}+1.257) * Jmax_{25,clim}$

SLA
The CO_2 responses of SLA was based on Poorter *et al.* (2009), where Pascal instead of ppm was used, therefore CO_2 is divided by 10. In addition, the LMA is converted to SLA.
C3-plants:

$SLA = SLA_{clim} / ((\exp(-0.251+0.008*(CO_{2,elev}/10)-0.000029*((CO_{2,elev} /10.\_dp)^2))) / (\exp(-0.251+0.008*(CO_{2,ref}/10)-0.000029*((CO_{2,ref}/10)^2))))$

C4-plants:

$SLA = SLA_{clim} / ((exp(-0.0651+0.00338*(CO_{2,elev}/10)-0.000039*((CO_{2,elev}/10)^2))) / (exp(-0.0651+0.00338*(CO_{2,ref}/10)-0.000039*(CO_{2,ref}/10)^2))))$

References: Ainsworth & Rogers (2007); Medlyn *et al.* (1999); Poorter *et al.* (2009)

S2 Time-series of changes in global carbon pools

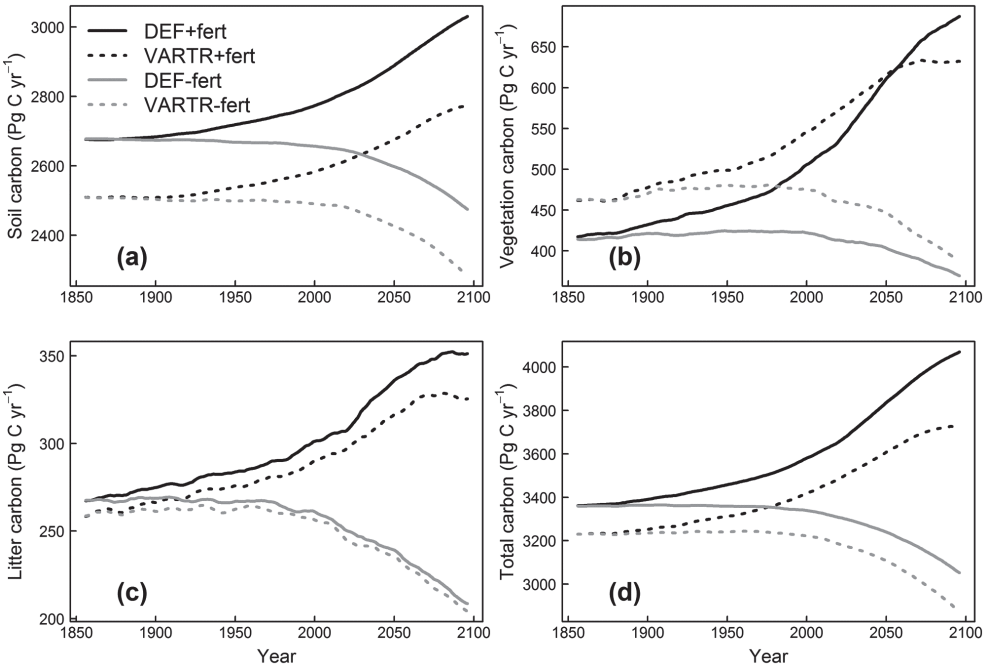

Figure S2. Change in global carbon pools (10-year running mean in Pg C yr^{-1}): a) soil carbon, b) vegetation carbon, c) litter carbon, d) total terrestrial carbon, sum of a,b and c. Note the different scaling on the y-axis.

S3 Time-series of changes in global mean carbon fluxes

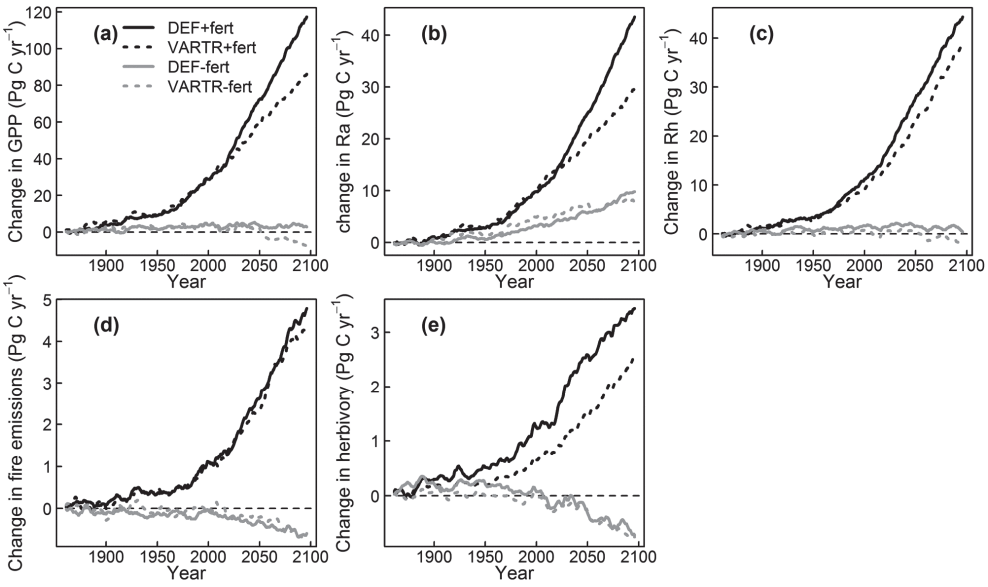

Figure S3. Change in global mean carbon fluxes (10-year running mean in Pg C yr^{-1}) compared to the mean of 1851-1860: a) GPP, b) Ra, c) Rh, d) fire emissions, e) herbivory. Positive values mean land carbon uptake. Note the different scaling on the y-axes.

S4 Latitudinal gradients of PFT-averaged traits

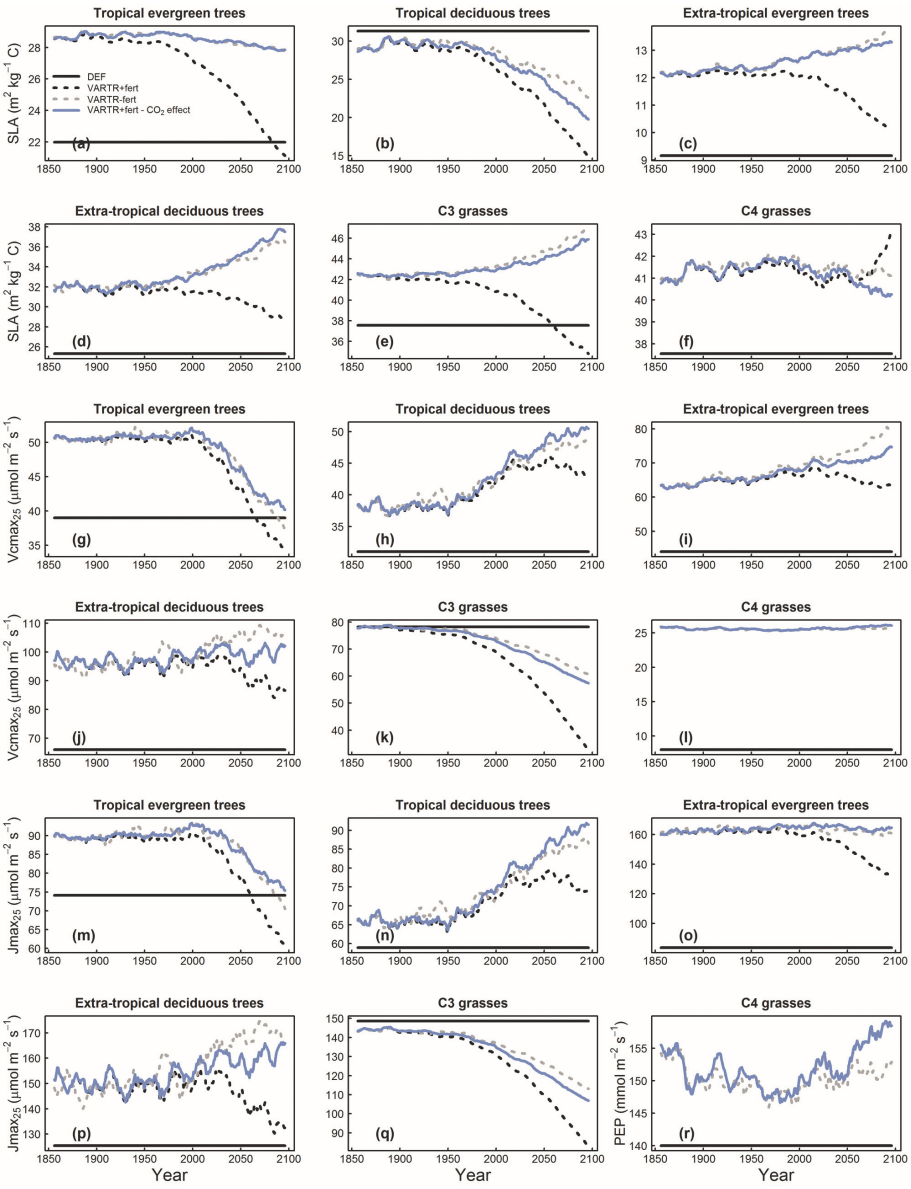

Figure S4. Changes in global mean traits (10-year running mean), weighted by fractional cover, of trees and grasses: a,g,m) tropical evergreen trees, b,h,n) tropical deciduous trees, c,i,o) extra-tropical evergreen trees, d,j,p) extra-tropical deciduous trees, e,k,q) C3-grasses, f,l,r) C4-grasses. Upper two rows SLA (kg m^{-2}), middle two rows $Vcmax_{25}$ (µmol m^{-2} s^{-1}), lower two rows $Jmax_{25}$ (µmol m^{-2} s^{-1}) with PEP (mmol m^{-2} s^{-1}) for C4-grasses. There was no CO_2 effect for C4-grasses and therefore lines of VARTR overlap. Note the different scaling on the y-axes.

S5 Latitudinal gradients of mean annual heterotrophic respiration

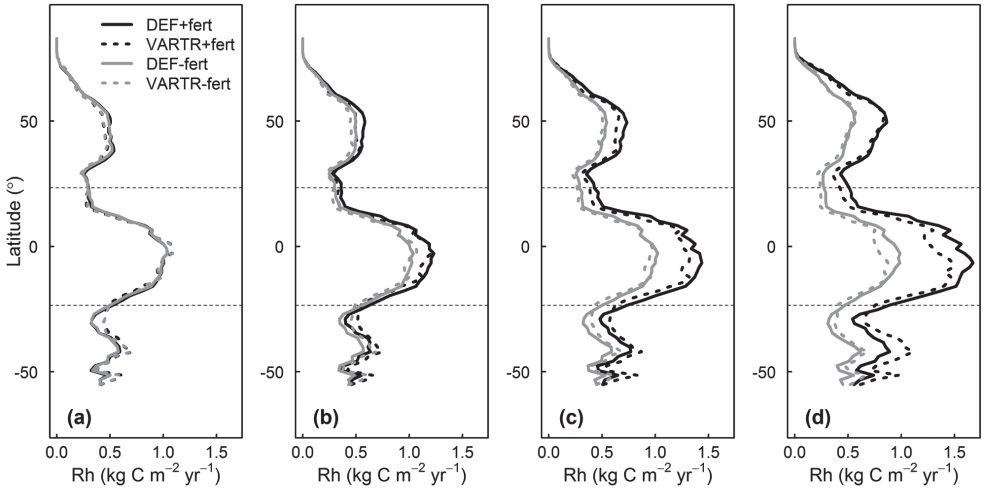

Figure S5. Latitudinal gradients of (10-year mean) average annual heterotrophic respiration (kg m^{-2} yr^{-1}): a) 1851, b) 2000, c) 2050, d) 2100. Horizontal dashed lines denote the Tropic of Cancer and Capricorn.